CrossMark

Future predictions of precipitation and temperature in Iraq using the statistical downscaling model

Mustafa Al-Mukhtar[1] · Mariam Qasim[1,2]

Abstract

Iraq is facing a critical water crisis that has ever experienced. This necessitates a wise management for present and future water resources. Future water availability is mainly influenced by the impacts of climate changes and to dams in Turkey, Syria, Iran, and northern Iraq. The meteorological parameters obtained from global circulation models (GCM) cannot be used to assess the impacts of future climate changes on the water resources availability at catchment scale. The dynamical or statistical downscaling is employed to transfer the coarse resolution of GCM into a finer. In this study, the future maximum/minimum temperature and precipitation for 12 stations of Iraq were projected for three future periods 2020s (2011–2040), 2050s (2041–2070), and 2080s (2071–2100) from the Canadian GCM model (CanESM2) under different scenarios (RCP2.5, RCP4.5, and RCP8.5) using statistical downscaling model (SDSM). The model was set up utilizing partial correlation and significance level of 0.05 between National Center for Environmental Prediction/Atmospheric Research (NCEP/NCAR) parameters as predictors and the local station data as predictand. Subsequently, the model was calibrated and validated against daily data by using 70% of the data for calibration and the remaining 30% for the validation. Thereafter, the calibrated model was applied to downscale future scenarios of CanESM2 predictors. The study proved a satisfactory performance of SDSM for simulation of maximum-minimum temperatures and precipitation for future periods. All considered stations and the scenarios were consistent in predicting increasing trend of maximum-minimum temperature and decreasing trend of precipitations. RCP8.5 scenario shows the worst trend of precipitation and temperature.

Keywords Statistical downscaling · Projections · Precipitation · Temperature · Iraq

Introduction

Due to human interventions and the use of fossil fuels, the greenhouse gas concentration in the atmosphere has increased and resulted in a global energy disparity (Wentz et al. 2007; Chu et al. 2010; Huang et al. 2011). This in turn has led to what is called climate changes. Change in the climate means a state within a certain period where the statistical distribution of weather patterns is changeable due to the radiative forcing (RF) variations (Al-Mukhtar 2018; Moussa et al. 2018). The sources of these variations arise from the natural, anthropogenic, and environmental process, which influence on the earth's energy budget (Khadka and Pathak 2016). The RFs are embedding to the climate models as boundary conditions to simulate future scenarios. The total anthropogenic RF was estimated according to IPCC Fifth Assessment Report (AR5) in 2011 as "43 % higher than that reported in the fourth Assessment Report (AR4) published in 2007" (IPCC 2013).

Iraq was characterized as an abundant water resources country among the other regional countries with an annual allocation per capita of 6029 m^3 in 1995; however, a significant drop was recorded in the annual allocation to become 2100 m^3 in 2015 (Nimah 2008). Restoration project for the marshes in the south of Iraq and the increasing demand on water in the neighboring countries will result in desiccation the Tigris and Euphrates Rivers in 2040 (Al-Ansari et al. 2012). This would in turn lead to some ecological and environmental consequences not only in Iraq but also on the Arabian/Persian Gulf and Kuwait (Al-Ghadban et al. 1999, 2008). Some suggested solutions to overcome the water

✉ Mustafa Al-Mukhtar
   mmalmukhtar@gmail.com

1 Civil Engineering Department, University of Technology-Baghdad, Baghdad, Iraq

2 Department of Civil Engineering, Al-Kufa University, Najaf, Iraq

shortage crises, but not only, are to use non-conventional water resources management techniques (e.g., water harvesting) (Al-Ansari et al. 2012; Zakaria et al. 2013) and by attending a mitigation and adaptation of climate change.

In order to adopt such strategies and to avoid ill-informed decisions about the prospective water resources availability, planners need knowledge about the impacts of climate changes on meteorological parameters at local scale. The global climate models (GCMs) are the main informative tools used for present and future climate change scenarios. However, the resolution of the GCMs is very coarse (usually more than 40,000 km^2), and thus, they are unable to accurately model the sub-grid scale climate features of the local-scale areas (Wilby and Dawson 2007). Thus, there is a need for spatial and temporal downscaling from the GCM into a finer scale.

Downscaling technique is defined as the tool to create a link between a regional/local and GCM scales (Wetterhall et al. 2009). The range of local and regional scales is 0–50 km and 50 × 50 km, respectively (Xu 1999). Downscaling can be grouped into two categories: dynamic and statistical downscaling (Christensen et al. 1997; Fowler et al. 2007). Dynamical downscaling (DD) is a process-based technique focused on driving nested high-resolution circulation model called regional climate model (RCM). This model takes the boundary conditions from the coarse resolution data of GCMs and provides information on fine temporal and spatial resolution that able to simulate the physical processes (Giorgi 1990; Jones et al. 1995). On the contrary, statistical downscaling (SD) methods associate local-scale with large-scale variables through empirical/ statistical relationship by using multiple linear regression and the stochastic weather generator (Gebremeskel et al. 2005; Diaz-Nieto and Wilby 2005; Gagnon et al. 2005; Wilby et al. 2006). Although these methods are characterized as faster, and computationally inexpensive (Wilby et al. 2000), they have shortcomings represented by assuming a constancy of the statistical association in the future.

Weather generators are stochastic models employed in SD methods to synthetically generate a long series data, reproduce missing data, and synthesize different realizations of the same data through a random number generator (Wilks and Wilby 1999). Statistical downscaling model (SDSM) is being widely used throughout the world as a statistical downscaling tool (Huang et al. 2011) to downscale most of climate variables (such as temperature, precipitation, and evaporation) which could be used in further assessing of hydrologic responses.

The objectives of this study were to investigate the ability of statistical downscaling model in reproducing the meteorological parameters (i.e., precipitation and temperature) and, hence, to analyze the impact of future climate changes (2011–2100) on precipitation and temperatures in several station of Iraq. To this end, the SDSM was calibrated and validated against daily observations from 12 stations scattered from the north to the south using NCEP/NCAR parameters. Then, the calibrated model was applied to project future precipitation and temperature over three time slices using the Canadian GCM. The outcomes from this study would help decision makers and researchers in better planning for the water resources in Iraq and help in finding ways and means to reduce the effects of climate changes on the inhabitants and the environment.

Study area and data description

Iraq occupies a total area of 437,072 km^2. Landforms constitute 432,162 km^2, while water forms 4910 km^2 of the total area. Turkey borders Iraq from the north, Iran from the east, Syria and Jordan from the west, and Saudi Arabia and Kuwait from the south. The total population in Iraq in 2017 is about 37,139,519. Iraq is composed of 18 governorates. Twelve sites were selected across Iraq to represent as much as possible major climatic regions in the country (Fig. 1). As such, the selected stations extend from the north to the south of the country where most of the agricultural and urban areas are present. The investigated stations are Baghdad, Kirkuk, Mosul, Sulaymaniyah, Najaf, Nasiriyah, Al-Hay, Basra, Zakho, Erbil, Salah ad Din, and Khanaqin. Table 1 presents a detail description about the locations of the investigated stations.

The observed data of those stations were obtained from the Iraqi National Meteorological Organization and Seismology. The data availability is listed in Table 2 with their corresponding mean annual precipitation and temperature. The observed daily rainfall and temperature data of the stations Kirkuk, Mosul, Baghdad, Nasiriyah, Najaf, Al-Hay, Basra, and Khanaqin were available for the period 1961–1990. While for the remainder stations (Sulaymaniyah, Zakho, Erbil, and Salah ad Din), the data were from 1971 to 2000. For better understanding of the climate behavior in those stations, the mean monthly precipitation and temperature were depicted as shown in Fig. 2. As it can be seen from the figure, the mean monthly precipitation of the 12 stations over the respective period ranged from 700 to 50 mm in January to zero in the summer months (Jun, July, August) and September. On the other side, the mean monthly temperature fluctuated from 45 to 30 °C in summer to 20–5 °C in winter. The climate is classified as arid in south to semi-arid in the north.

The 26 predictors of NCEP/NCAR reanalyzed predictors with grid resolution 2.5° × 2.5° were freely downloaded from (https://www.esrl.noaa.gov/psd/data/reanalysis/reanalysis.shtml). These predictors represent the observed coarse resolution parameters of past to present time.

Fig. 1 Location of the meteorological stations
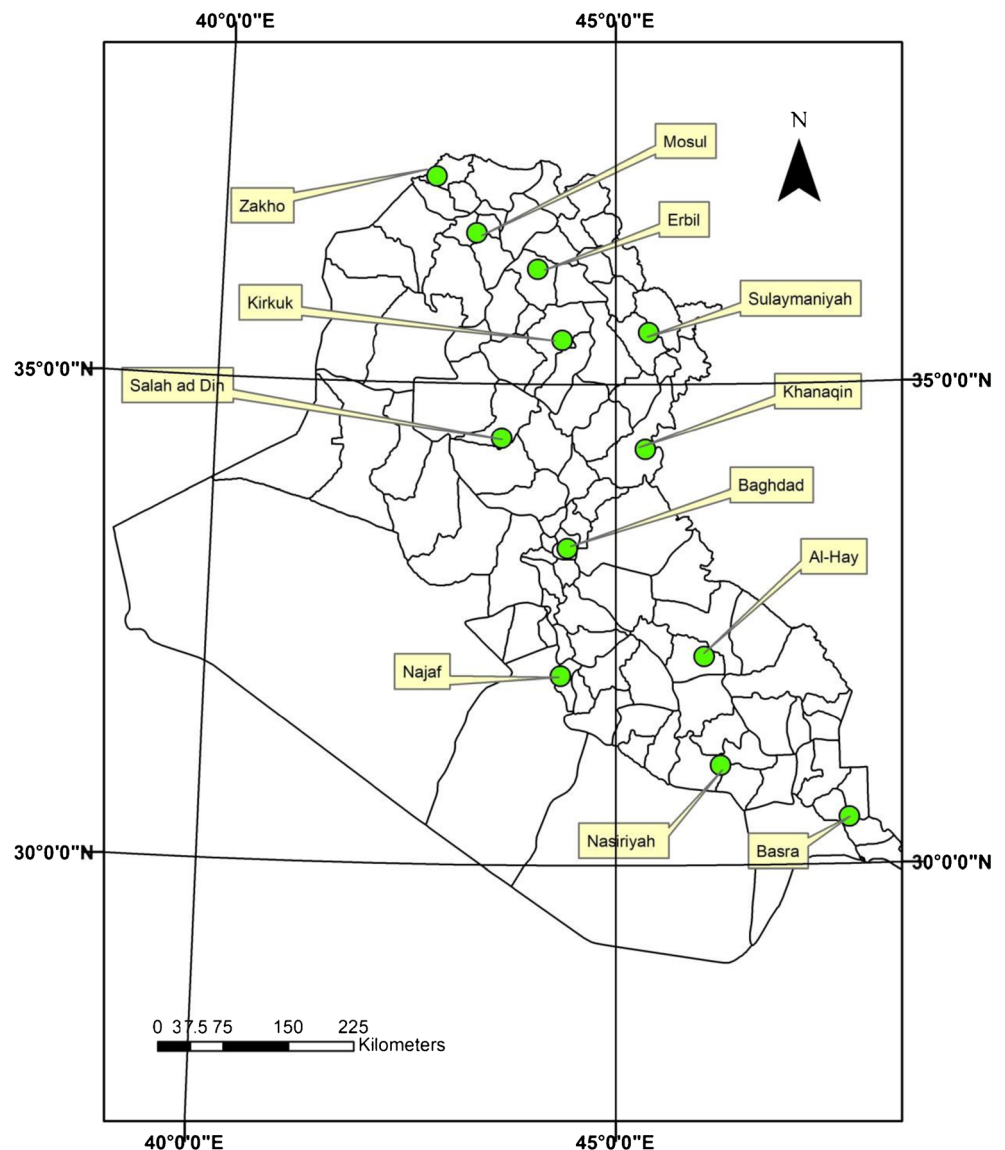
The CMIP5-ESMs climate model of the Canadian model for a very high emission (RCP8.5), an intermediate emission (RCP4.5), and very low emission (RCP2.6) scenarios with grid resolution 2.8125° × 2.8125° were obtained from the Canadian Centre for Climate Modeling and Analysis (http://climate-scenarios.canada.ca/?page=pred-canesm2) for the periods of 1961–2001 and 1961–2099. These predictors are available in zip file format and encompass five files inside: CanESM2_historical_1961–2005, CanESM2_rcp2.6_2006–2100, CanESM2_rcp4.5_2006–2100, CanESM2_rcp8.5_2006–2100, and NCEP-NCAR_1961–2005. Due to the presence of inconsistency between the GCM and NCEP resolutions, the NCEP data were interpolated to be consistent with the data grid resolution of CanESM2. The above variables with those from observations were used for calibration, validation, and projection in SDSM.

Methodology

The SDSM

The statistical downscaling was carried out by SDSM. The model was downloaded from http://www.sdsm.org.uk. Wilby et al. (2002) developed the model as a hybrid tool of both the multiple linear regression (MLR) and the stochastic weather generator (SWG). The rule of MLR is to establish a statistical/empirical relationship between large-scale and local-scale variables, and make some regression parameters from the present data. In order to establish a better association with the observed time series, the calibrated parameters from MLR along with NCEP and GCM predictors are fed into SWG to simulate up to 100 daily time series (Wilby et al. 2002; Liu et al. 2009).

Table 1 Location details of the 12 stations in Iraq

Station	Latitude	Longitude	Altitude (m)	Area (km^2)	Population
Bagdad	33° 18′ N	44° 24′ E	34	204.2	7,665,000
Basra	30° 31′ N	47° 47′ E	5	181	2,150,000
Erbil	36° 11′ 28″N	44° 0′ 33″ E	390	197	852,500
Al-Hay	32° 10′ N	46° 03′ E	20	–	84,800
Najaf	32° N	44° 20′ 00″ E	60	28,824	1,389,500
Nasiriyah	31° 03′ N	46° 16′E	9	12,900	860,200
Zakho	37° 08′ 37 N	42° 40′ 54.88″ E	440	–	350,000
Sulaymaniyah	35° 33′ N	45° 25′E	882	20,144	1,256,000
Salah ad Din	34° 27′ N	43° 35′E	–	24,751	1,408,000
Khanaqin	34° 20′ N	45° 23′E	183	–	150,000
Mosul	36.34° N	43.13° E	223	180	664,221
Kirkuk	35° 28′ N	44° 19′ 0″ E	350	9679	850, 787

The selection of the most suitable predictors among the atmospheric predictors is done through a combination of statistical tools, i.e., correlation matrix, partial correlation, P value, histograms, and scatter plots. The calibrated parameters are optimized through either ordinary least squares (OLS) or dual simplex (DS) (Huang et al. 2011). The model determines the relationship between the predictands and predictors through three kinds of sub-models—monthly, seasonal, and annual. Annual sub-model derives one-regression parameters for 12 months. While, the monthly sub-model represents 12 regression equations of the 12 months. Moreover, conditional and unconditional processes are applied within the model for precipitation and temperature, respectively (Wilby et al. 2002; Chu et al. 2010), where the conditional process depends on an intermediate variable to link the predictors with predictands, while the unconditional process considers the direct link between them (Khan et al. 2006). The methodology followed in this study for downscaling and scenario generation is shown in Fig. 3.

Screening of probable predictors

One of the most important steps in statistical downscaling is to identify properly the most effective predictors on predictands in what is called screening of predictors (Hewitson and Crane 1996). This process is employed to select appropriate sets of observed predictors from the suite of NCEP/NCAR reanalysis datasets based on several statistical metrics. The choice of predictors differs based on geographical regions considering the properties of the predictor and the predictand (Anandhi et al. 2009). Therefore, in this study, the scatter plots, value of explained variance, correlation, partial correlation (r), and P value approaches were used for obtaining the most suitable sets of predictors from the suite of NCEP/NCAR data at an

Table 2 Description of data availability for the 12 stations used in the study

Station	Period	Data available	Mean annual precipitation (mm)	Mean annual Tmax (°C)	Mean annual Tmin (°C)
Baghdad	1961–1990	Temp. and prec.	31.1	28.5	15.8
Basra	1961–1990	Temp. and prec.	31.3	27.7	12.7
Erbil	1961–1990	Temp. and prec.	11.8	30.3	14.6
Al-Hay	1971–2000	Temp. and prec.	60.8	24.6	12.2
Najaf	1961–1990	Temp. and prec.	8.12	30.9	17
Nasiriyah	1961–1990	Temp. and prec.	9.5	31.7	17.32
Zakho	1961–1990	Temp. and prec.	60	31.6	16.9
Sulaymaniyah	1961–1990	Temp. and prec.	10.7	31.8	18.1
Salah ad Din	1971–2000	Temp. and prec.	52.9	25.3	12
Khanaqin	1971–2000	Temp. and prec.	34.6	25.7	14.6
Mosul	1971–2000	Temp. and prec.	50.2	21.44	12.5
Kirkuk	1961–1990	Temp. and prec.	25.5	30	14.9

Temp. temperature, *prec.* precipitation

Fig. 2 Monthly **a** temperature
and **b** precipitation at weather
stations for the baseline period
(1961–1990 and 1971–2000)
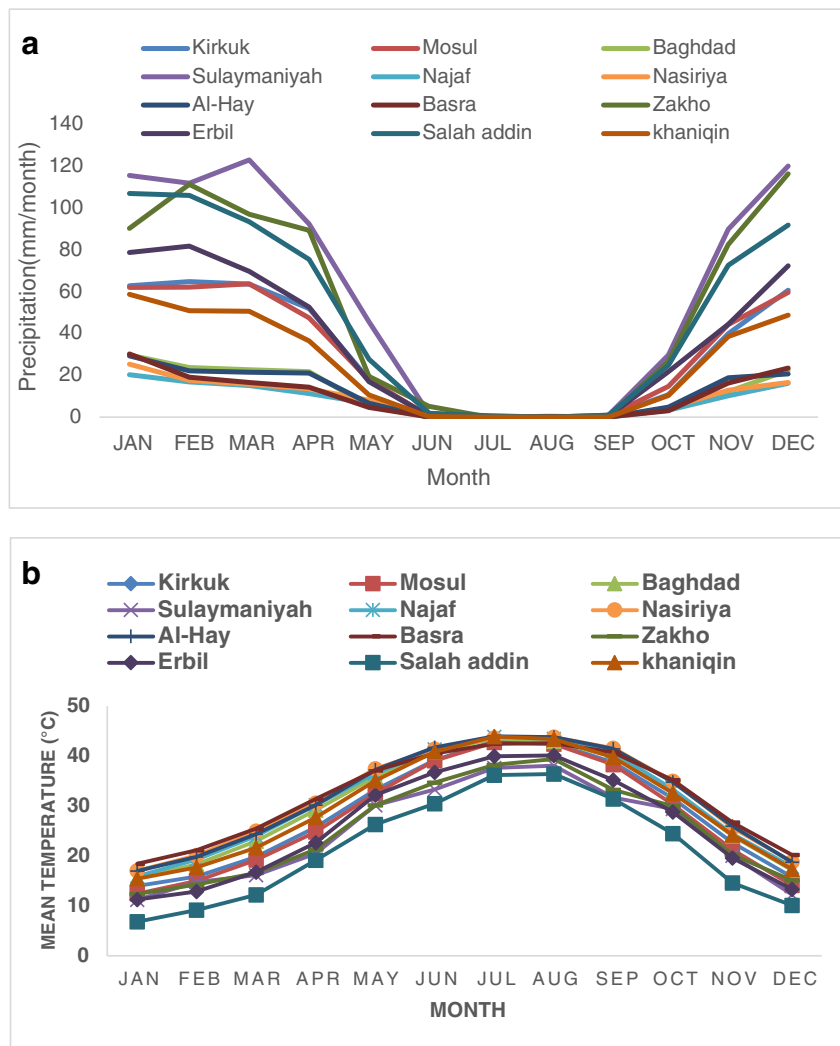
individual station. As pointed by Wilby et al. (2002), "the explained variance explains the level to which daily variations in the predictand are determined by predictors." While, the correlation statistics and P values are a measure of the strength of relationship between the predictor and predictand. The smaller P value ($P < 0.05$) implies a better association between variables.

Calibration and validation

Quality control check function was used to identify whether the data have missing or outlier values. The observed data in each station (predictands) with their NCEP/NCAR were used to calibrate and validate the model. Data was partitioned into two parts: 70% for calibration and 30% for validation. So, data from 1961 to 1981 and 1971 to 1991 was used for the calibration, where the model was calibrated with the screened NCEP predictors using the annual sub-models, for the respective predictands. The unconditional sub-model without transformation was used for temperature and conditional one with

fourth root transformation for precipitation. The OLS was adopted as an optimization method. Subsequently, daily dataset for the period of 1982–1990 and 1992–2000 was selected for the validation of each predictand. Validation was carried out using calibration output, and observed NCEP reanalyzed atmospheric variables. Then, SWG was employed to generate 20 ensembles of synthetic weather series. The average of these ensembles was compared with independent observations from the validation period.

Downscaling of future predictands

In this study, the calibrated model was used in further analysis, i.e., assessing future climate changes on temperature and precipitation over three periods by downscaling the RCP scenario predictors obtained from the CanESM2 model. To achieve that, the built-in SWG was employed to generate 20 ensembles of future predictands. Ultimately, the downscaled future climate change predictands in the 2020s (2011–2040), 2050s (2041–2070), and 2080s (2071–2099) were compared with
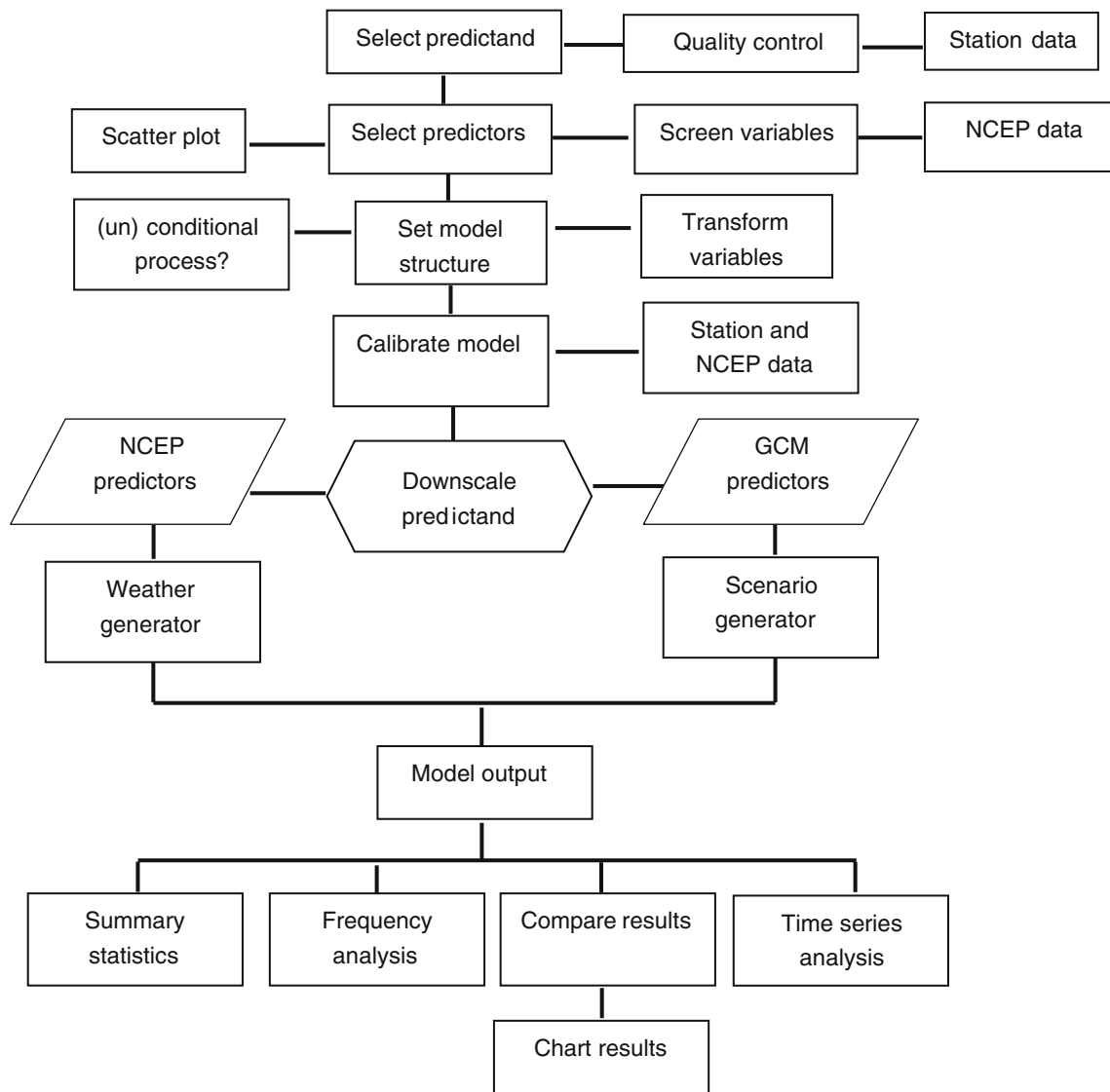
Fig. 3 Flow chart showing steps involved in downscaling and scenario generation (after Wilby and Dawson 2007)

those in the baseline period (1961–1990). The anomaly of monthly precipitation/temperature was obtained from the percentage change/absolute difference of average 20-ensemble future predictand with respect to monthly average of the baseline period. The positive or negative anomaly indicates that there would be increase or decrease of the variable in future periods, respectively.

Evaluation criteria

In order to evaluate the SDSM performance with respect to the observed Tmax, Tmin, and precipitation data, the following three statistical model performance evaluations were applied. These statistical performance measures are mostly used to check the goodness of fit between the observed and modeled (Al-Mukhtar 2016).

Coefficient of determination (R^2)

The determination coefficient or coefficient of determination (Eq. 1) is a measure used to determine the variability in observed data that the model could capture it (Krause et al. 2005).

$$R^2 = \frac{\left(\sum [X_i - X_{av}][Y_i - Y_{av}]\right)^2}{\sum (X_i - X_{av})^2 \sum (Y_i - Y_{av})^2} \qquad (1)$$

where Xi is measured value, X_{av} is average measured value, Y_i is simulated value, and Y_{av} is average simulated value.

Nash–Sutcliffe coefficient

The Nash–Sutcliffe coefficient (NSE) is a dimensionless model evaluation statistic where the relative magnitude of the

Table 3 Significant predictors from CanESM2 model for precipitation

Station	Predictor	P.r	P	Station	Predictor	P.r	P
Baghdad	ncepmslpgl	−0.013	0.0007	Erbil	ncepmslpgl	0.068	0.000
	ncepp1-fgl	0.002	0.0373		ncepp5-zgl	−0.001	0.000
	ncepp500-gl	0.028	0.0003		ncepp500-gl	−0.024	0.000
	nceps500-gl	−0.033	0.0017		ncepp850-gl	0.003	0.0001
	nceptempgl	−0.11	0.0343		ncepprcpgl	0.001	0.0442
					nceps850-gl	−0.018	0.000
					nceptempgl	0.0208	0.000
Basra	ncepmslpgl	−0.003	0.0005	Kirkuk	ncepp1-vgl	0.125	0.0025
	ncepp1-fgl	0.040	0.0419		ncepp500-gl	0.0354	0.00
	ncepp1-ugl	−0.051	0.033		ncepp8-vgl	0.007	0.0309
	ncepp1-zhgl	0.020	0.0342		ncepp850-gl	−0.044	0.0253
	ncepp500-gl	−0.018	0.0009		ncepp8-zhgl	−0.887	0.0014
	ncepp850-gl	0.019	0.0074		ncepprcpgl	−0.005	0.00
	nceps500-gl	−0.045	0.0005		nceps850-gl	0.125	0.0042
					nceptempgl	0.0154	0.0097
Zakho	ncepmslpgl	0.182	0.0022	Salah ad Din	ncepp1-vgl	0.005	0.0466
	ncepp5-zgl	0.365	0.0300		ncepp1-zgl	0.004	0.0297
	ncepp500-gl	0.006	0.000		ncepp500-gl	−0.007	0.00
	ncepp850-gl	0.005	0.0001		ncepp8-vgl	−0.124	0.0222
	precipitation	0.187	0.0442		ncepp8-zgl	−0.109	0.0198
	nceps850-gl	−0.009	0.0032		ncepp850-gl	0.006	0.00
	nceptempgl	−0.540	0.00				
Al-Hay	ncepmslpgl	−0.034	0.0003	Mosul	ncepp1-vgl	0.002	0.0466
	ncepp8-ugl	−0.098	0.0043		ncepp1-zgl	0.0233	0.0297
	ncepp850-gl	0.0523	0.0207		ncepp5-zgl	−0.124	0.00
	ncepp8-thgl	0.007	0.0371		ncepp500-gl	−0.0243	0.000
	nceps500-gl	0.002	0.0157		ncepp8-vgl	0.008	0.0222
	nceptempgl	0.0123	0.0140		ncepp8-zgl	−0.265	0.0198
					ncepp850-gl	0.007	0.000
					nceps850-gl	0.0998	0.000
Khanaqin	ncepmslpgl	0.148	0.00	Sulaymaniyah	ncepp1-vgl	−0.002	0.0052
	ncepp1-ugl	0.134	0.0346		ncepp500-gl	0.128	0.0032
	ncepp5-zgl	−0.2	0.0004		ncepp8-vgl	0.134	0.0208
	ncepp500-gl	−0.009	0.000		ncepp850-gl	0.003	0.0234
	ncepp8-vgl	0.129	0.0341		ncepp8-zhgl	−0.009	0.0123
	nceps850-gl	0.003	0.000		Precipitation	0.0176	0.00
	nceptempgl	0.0345	0.000		nceps850-gl	0.0034	0.0042
Najaf	ncepmslpgl	−0.006	0.0044	Nasiriyah	ncepmslpgl	−0.0004	0.0007
	ncepp500-gl	−0.028	0.0008		ncepp500-gl	0.006	0.0104
	ncepp8-zgl	0.006	0.004		nceps850-gl	0.145	0.0062
	nceps850-gl	0.125	0.0477		nceptempgl	0.134	0.0014

ncepmslpgl: mean sea-level pressure, ncepp8-fgl: 850-hpa airflow strength, ncepp1-fgl: 1-hpa airflow strength, ncepp8-ugl: 850-hpa zonal velocity, ncepp1-ugl: 1-hpa zonal velocity, ncepp8-vgl: 850-hpa meridional velocity, ncepp1-vgl: 1-hpa meridional velocity, ncepp8-zgl: 850-hpa vorticity, ncepp1-zgl: 1-hpa vorticity, ncepp8-thgl: 850-hpa wind direction, ncepp1-thgl: 1-hpa wind direction,ncepp8-zhgl: 850-hpa divergence, ncepp1-zhgl: 1-hpa divergence, ncepp500-gl: 500-hpa geopotential height, ncepp5-fgl: 500-hpa airflow strength, ncepp850-gl: 850-hpa geopotential height, ncepp5-ugl: 500-hpa zonal velocity, ncepprcpgl: precipitation, ncepp5-vgl: 500-hpa meridional velocity,nceps500-gl: specific humidity at 500 hpa, ncepp5-zgl: 500-hpa vorticity, nceps850-gl: specific humidity at 850 hpa, ncepp5-thgl: 500-hpa wind direction, ncepshumgl: surface-specific humidity, ncepp5-zhgl: 500-hpa divergence, nceptempgl: mean temperature at 2 m

Table 4 Statistical performance of Tmax modeling during calibration

Station name	RMSE	R^2	NSE
Baghdad	5.57	0.89	0.74
Basra	5.40	0.89	0.73
Erbil	5.53	0.88	0.76
Al-Hay	5.22	0.89	0.73
Khanaqin	5.13	0.89	0.77
Kirkuk	4.68	0.89	0.81
Mosul	5.23	0.88	0.78
Najaf	5.22	0.83	0.75
Nasiriya	5.26	0.90	0.72
Salah ad Din	5.57	0.83	0.74
Zakho	5.09	0.88	0.78
Sulaymaniyah	5.32	0.81	0.73

Table 6 Statistical performance of Tmin modeling during calibration

Station name	RMSE	R^2	NSE
Baghdad	4.56	0.83	0.89
Basra	4.53	0.83	0.69
Erbil	4.29	0.84	0.73
Al-Hay	4.31	0.85	0.71
Khanaqin	4.21	0.83	0.73
Kirkuk	3.87	0.83	0.79
Mosul	4.37	0.87	0.72
Najaf	4.47	0.85	0.73
Nasiriya	4.25	0.80	0.71
Salah ad Din	4.26	0.83	0.89
Zakho	4.33	0.85	0.88
Sulaymaniyah	4.50	0.87	0.72

residual variance is determined in comparison to the observed variance (Moriasi et al. 2007) and is defined as the following (Nash and Sutcliff 1970):

$$E = 1 - \frac{\sum_{i=1}^{n}(X_i - Y_i)^2}{\sum_{i=1}^{n}(X_i - Y_{av})^2}. \tag{2}$$

Root mean square error

The root mean square error (RMSE) is an error index type of model evaluation statistics (dimensional). The closer value to zero, the better model performance (Singh et al. 2004).

$$RMSE = \sqrt{\frac{\sum_{i=1}^{n}(X_i - Y_i)^2}{n}} \tag{3}$$

where n is the number of values.

Results

Screening of predictors

The best-correlated predictor variables were selected based on P value and partial r for each station's predictands. Results revealed that different atmospheric variables affect different local variables. The driving parameters on Tmax and Tmin with significance level < 0.05 were common. In other words, ncepp500-gl (500-hpa geopotential height), nceps850-gl (specific humidity at 850 hpa), ncepshumgl (surface-specific humidity), and nceptempgl (mean temperature at 2 m) were the most effective parameters on temperature at all stations. These parameters seem physically rational because they are highly related to the changes of temperature characteristics through the thermal advection term (Romanowicz et al. 2016). While, the driving parameters on precipitation were varied across the stations (Table 3). For example, in Baghdad station, the most significant parameters were ncepmslpgl (mean sea-level pressure), ncepp1-fgl (1-hPa air flow strength), ncepp500-gl (500-

Table 5 Statistical performance of Tmax modeling during validation

Station name	RMSE	R^2	NSE
Baghdad	5.34	0.90	0.75
Basra	5.45	0.90	0.74
Erbil	5.69	0.87	0.75
Al-Hay	5.40	0.90	0.74
Khanaqin	5.39	0.89	0.77
Kirkuk	4.65	0.89	0.83
Mosul	5.56	0.84	0.77
Najaf	5.31	0.78	0.74
Nasiriya	5.51	0.89	0.72
Salah ad Din	6.67	0.78	0.67
Zakho	5.43	0.87	0.72
Sulaymaniyah	5.86	0.90	0.74

Table 7 Statistical performance of Tmin modeling during validation

Station name	RMSE	R^2	NSE
Baghdada	4.50	0.84	0.69
Basrah	4.45	0.84	0.70
Erbil	4.53	0.82	0.73
Al-Hay	4.55	0.87	0.71
Khaniqin	4.70	0.84	0.72
Kirkuk	3.86	0.84	0.82
Mosul	4.36	0.87	0.74
Najaf	4.50	0.84	0.74
Nasiriya	4.62	0.76	0.71
Salah ad Din	5.25	0.84	0.99
Zakho	4.22	0.82	0.73
Sulaymaniyah	4.20	0.82	0.87

Table 8 Statistical performance of precipitation modeling during calibration

Station name	RMSE	R^2	NSE
Baghdada	0.77	0.71	0.64
Basrah	0.84	0.86	0.72
Erbil	0.95	0.60	0.64
Al-Hay	0.39	0.67	0.76
Khaniqin	0.34	0.80	0.82
Kirkuk	0.44	0.61	0.87
Mosul	0.36	0.62	0.86
Najaf	0.49	0.59	0.61
Nasiriya	0.73	0.70	0.67
Salah ad Din	0.37	0.51	0.60
Zakho	0.47	0.61	0.85
Sulaymaniyah	0.34	0.62	0.87

hPa geopotential height), nceps500-gl (specific humidity at 500 hPa), and nceptempgl (mean temperature at 2 m). Whereby, in Basra south of Iraq, in addition to the above parameters, the most significant parameters were ncepp1-ugl (1-hPa zonal velocity), ncepp1-zhgl (1-hPa divergence), and ncepp850-gl (850-hPa geopotential height). The reason behind such as variation might be attributed due to the precipitation heterogeneity (Wilby et al. 2002). The most effective parameters on precipitation in most of stations were the specific and relative humidity. These parameters are associated and highly correlated to precipitation occurrence because their synchronous variation is dependent on the saturated phase of water vapor in the air (Hessami et al. 2008). The significant deriving parameters were subsequently used in the SDSM calibration.

Calibration and validation

Based on station data availability, the observed data was either from 1961 to 1990 or 1971–2000. This data was

Table 9 Statistical performance of precipitation modeling during validation

Station name	RMSE	R^2	NSE
Baghdada	0.79	0.61	0.74
Basrah	0.57	0.55	0.65
Erbil	0.83	0.62	0.82
Al-Hay	0.77	0.86	0.80
Khaniqin	1.01	0.80	0.78
Kirkuk	0.37	0.63	0.63
Mosul	0.39	0.83	0.60
Najaf	0.74	0.61	0.86
Nasiriya	0.86	0.63	0.70
Salah ad Din	0.88	0.84	0.66
Zakho	0.54	0.64	0.76
Sulaymaniyah	0.45	0.67	0.70

portioned into two parts: for calibration and validation. Data from 1961 to 1981 and 1971 to 1991 was used for the calibration, whereas data from 1982 to 1990 and 1992–2000 was used for the validation of the model. The statistical performance of calibration and validation results for the 12 spatial stations between the observed Tmax and those counterparts from the downscaling model are listed in Tables 4 and 5, respectively.

It can be noticed from Table 4 that the RMSE, R^2, and NSE were ≤ 5.57 °C, ≥ 0.80, and ≥ 0.70, respectively, across all the stations. According to the RMSE values, Kirkuk station has the lowest value (4.65 °C) among the other stations. In overall, results proved a well performance of SDSM in modeling maximum temperature during the calibration period. Thus, those results can be used in further analysis, i.e., validation phase. During the validation period, the statistical performance was almost akin to that in the calibration. The values of RMSE, R^2, and NSE were ≤ 6.67 °C, ≥ 0.78, and ≥ 0.67 across all the stations (Table 5) with the lowest RMSE in Kirkuk station as well. Therefore, it can be concluded that the performance of the calibrated model was representative for the entire data set and, thus, can be used in future projection.

Tables 6 and 7 list the statistical evaluation performances of Tmin predictand during the calibration and validation, respectively. It can be noticed from Table 6 that the RMSE, R^2, and NSE were ≤ 4.56 °C, ≥ 0.83, and ≥ 0.69, respectively, across all the stations during the calibration. According to this evaluation, it can be judged that the observed and the modeled data were consistent. In other words, the SDSM were sufficiently capable to reproduce the observed Tmin data. During the validation period, the values of RMSE, R^2, and NSE were ≤ 5.25 °C, ≥ 0.76, and ≥ 0.69 across all the stations, respectively (Table 7). Thus, the calibrated model could be used for future projections with respect to minimum temperature.

With respect to precipitation modeling, the performance evaluation shows that the observed and the modeled data were close to each other. The values of the RMSE, R^2, and NSE were ≤ 0.95 mm, ≥ 0.51, and ≥ 0.60, respectively, across all the stations during the calibration period (Table 8). Therefore, it can be concluded that the model's performance was satisfactory in presenting a rather well correlation between both data sets and subsequently was used in the validation phase. The values of statistical performance evaluation during the validation are listed in Table 9. RMSE, R^2, and NSE were ≤ 1.01 mm, ≥ 0.55, and ≥ 0.60, respectively, across all the stations. Thus, the SDSM was efficiently capable to reproduce the observed precipitation data in such as arid and semi-arid areas.
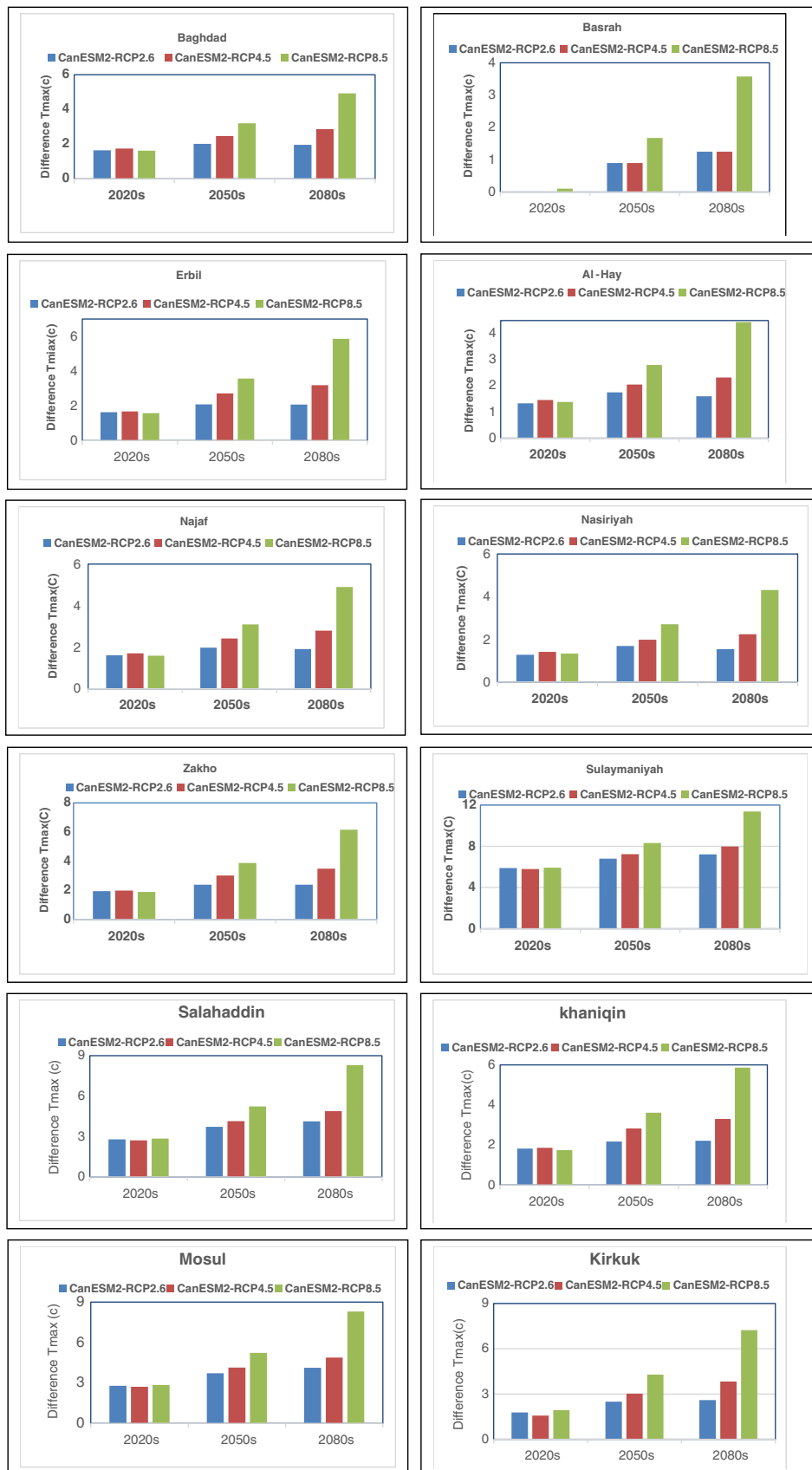
Fig. 4 Change in average annual maximum temperature in the future under CanESM2-RCP2.6, CanESM2-RCP4.5, and CanESM2-RCP8.5 scenarios
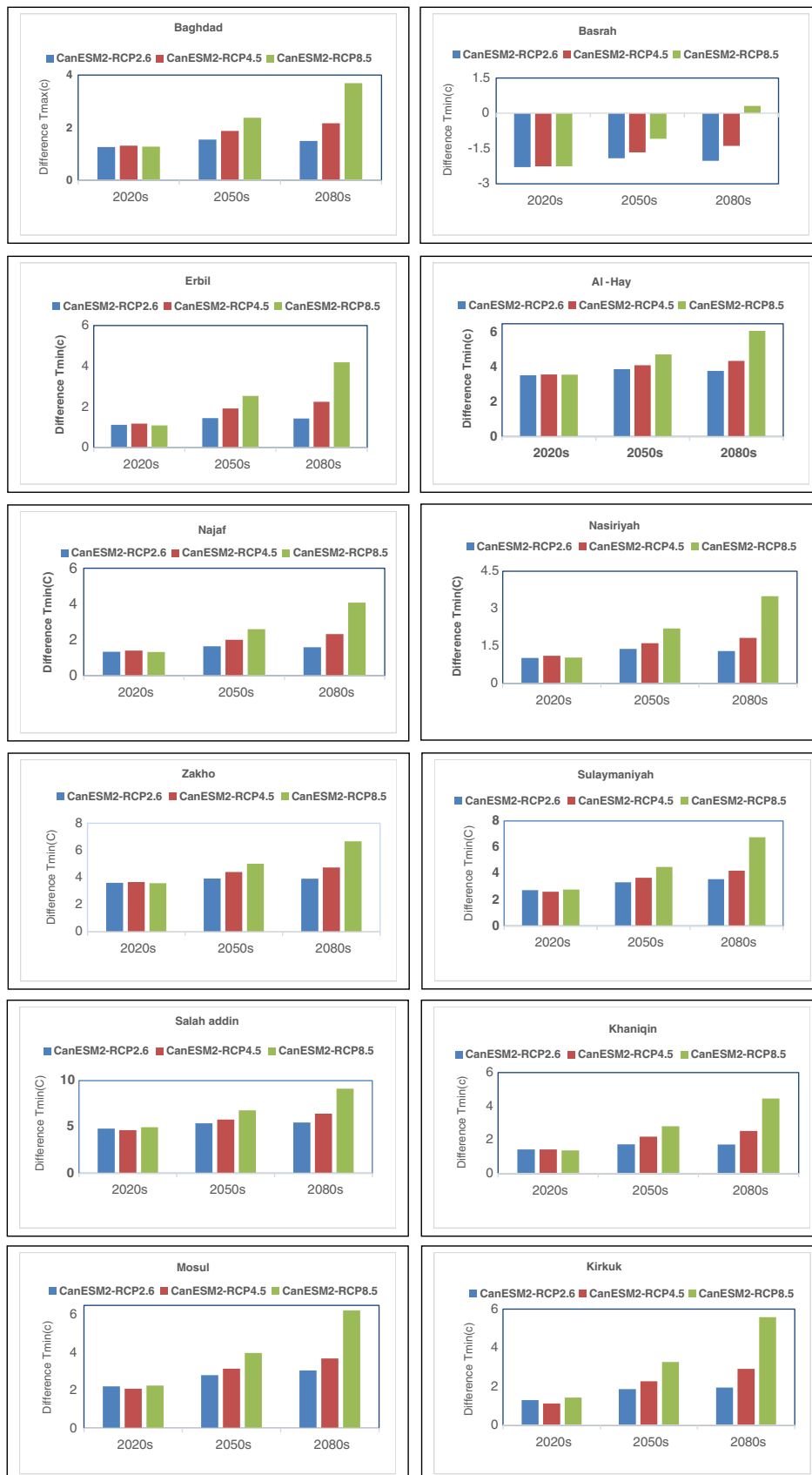
Fig. 5 Change in average annual minimum temperature in the future under CanESM2-RCP2.6, CanESM2-RCP4.5, and CanESM2-RCP8.5 scenarios
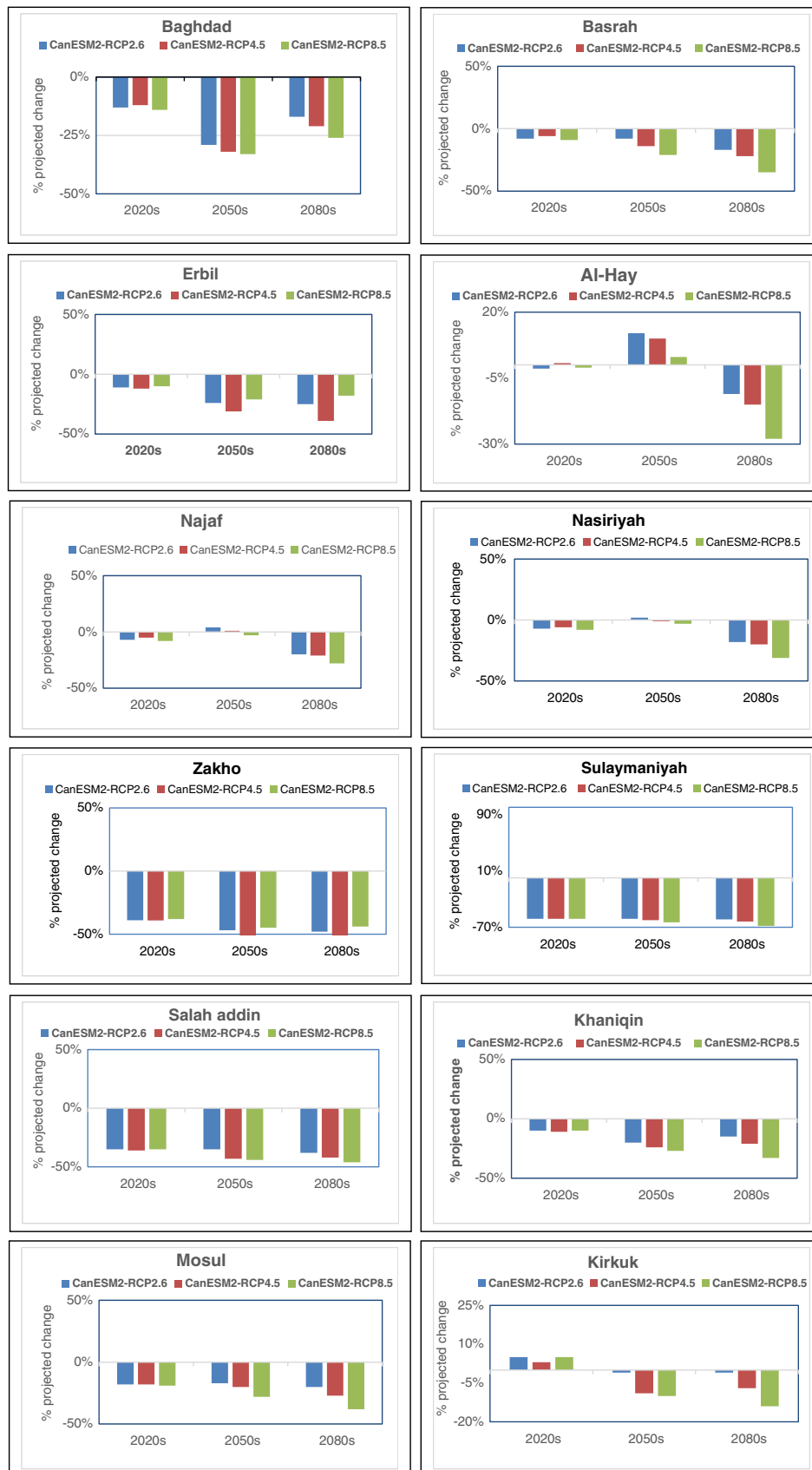
Fig. 6 Change in average annual rainfall in the future under CanESM2-RCP2.6, CanESM2-RCP4.5, and CanESM2-RCP8.5 scenarios

Table 10 Anomaly of maximum temperature (°C) from RCP scenarios over first, second, and third periods relative to baseline

Station	2011–2040			2041–2070			2071–2100		
	RCP2.6	RCP4.5	RCP8.5	RCP2.6	RCP4.5	RCP8.5	RCP2.6	RCP4.5	RCP8.5
Baghdad	1.6	1.7	1.62	2.02	2.47	3.2	1.9	2.8	4.9
Basrah	0.004	0.005	0.105	0.89	0.89	1.6	1.24	1.24	3.57
Erbil	1.6	1.67	1.5	2.08	2.7	3.5	2.07	3.1	5.8
Al-Hay	1.3	1.4	1.3	1.7	2	2.7	1.6	2.3	4.4
Najaf	1.6	1.7	1.5	1.97	2.4	3	1.91	2.7	4.8
Nasiriyah	1.2	1.4	1.3	1.6	1.9	2.7	1.53	2.3	4.3
Zakho	1.94	1.96	1.89	2.39	3.02	3.88	2.38	3.49	6.16
Sulaymaniyah	5.8	5.7	5.9	6.8	7.2	8.3	7.2	7.9	11.3
Salah ad Din	3.7	2.7	3.8	1.7	4.1	5.4	4.1	4.6	8.2
Al-Mosul	2.7	2.7	2.8	3.7	4.1	5.2	4.1	4.8	8.2
Khanaqin	1.8	1.8	1.7	2.1	2.8	3.6	2.2	3.2	5.8
Kirkuk	1.7	1.5	1.9	2.4	3	4	2.5	3.8	7

In general, the downscaled temperature and precipitation values were closely consistent with the observed. Many previous studies (Hassan et al. 2014; Yang et al. 2012, and many others) have demonstrated that the downscaling can better reproduce temperature series than precipitation. However, we conclude that the SDSM is powerful in reproducing predictand values and, therefore, the model efficiently downscaled the maximum-minimum temperature and precipitation during the calibration and validation periods.

Downscaling future climate scenarios

The SDSM model developed for each site was used to predict future daily precipitation and temperature in the sites for the periods of 2011–2040, 2041–2070, and 2071–2100

(hereinafter first, second, and third periods, respectively) based on the RCP2.6, RCP4.5, and RCP8.5 scenarios generated from CanESM2. Side-by-side anomaly results for all the meteorological stations of the three different scenarios are plotted as shown in Figs. 4, 5, and 6 for Tmax, Tmin, and precipitation, respectively, projected by the SDSM model under the three future periods. Tables 10, 11, and 12 tabulate the anomaly values of Tmax, Tmin, and precipitation, respectively, projected by the SDSM model under the three future periods. As it can be noticed, the maximum temperature was projected to increase across all the 12 stations with a minimum increase of 0.04 °C under RCP2.6 in Basra during the first period and maximum increase of 11.3 °C under RCP8.5 in Sulaymaniyah during the third period (Table 10 and Fig. 4). The minimum temperature was also projected to increase in

Table 11 Anomaly of minimum temperature (°C) from RCP scenarios over first, second, and third periods relative to baseline

Station	2011–2040			2041–2070			2071–2100		
	RCP2.6	RCP4.5	RCP8.5	RCP2.6	RCP4.5	RCP8.5	RCP2.6	RCP4.5	RCP8.5
Baghdad	1.26	1.3	1.27	1.54	1.87	2.3	1.5	2.1	3.6
Basrah	− 2.2	− 2.25	− 2.25	− 1.9	− 1.66	− 1.08	− 2.02	− 1.3	0.3
Erbil	1.1	1.1	1	1.4	1.9	2.5	1.4	2.2	4.8
Al-Hay	3.5	3.5	3.5	3.8	4.1	4.7	3.7	4.3	6
Najaf	1.3	1.4	1.3	1.6	2	2.6	1.5	2.3	4
Nasiriyah	1	1	1	1.3	1.6	2	1.2	1.8	3.5
Zakho	3.6	3.66	3.5	3.93	4.4	5.02	3.91	4.7	6.6
Sulaymaniyah	2.7	2.6	2.7	3.3	3.6	4.4	3.5	4.2	6.7
Salah ad Din	2.2	2.5	2.2	2.8	3	3.9	3	3.6	6.2
Al-Mosul	2.2	2	2.2	2.8	3	3.9	3	3.6	6.2
Khanaqin	1.4	1.4	1.3	1.4	2.1	2.8	1.7	2.5	4.4
Kirkuk	1.2	1.1	1.4	1.8	2.2	3.2	1.9	2.9	5.5

Table 12 Anomaly of precipitation (%) from RCP scenarios over first, second, and third periods relative to baseline

Station	2011–2040			2041–2070			2071–2100		
	RCP2.6	RCP4.5	RCP8.5	RCP2.6	RCP4.5	RCP8.5	RCP2.6	RCP4.5	RCP8.5
Baghdad	− 13	− 12	− 14	− 29	− 32	− 33	− 17	− 21	− 26
Basrah	− 8	− 6	− 9	− 8.4	− 14	− 21	− 17	− 22	− 35
Erbil	− 11	− 11	− 10	− 24	− 31	− 21	− 25	− 39	− 18
Al-Hay	− 1	0.7	− 1	− 1.2	− 1	− 3	− 1.1	− 1.5	− 2.75
Najaf	− 7	− 5	− 8	− 4	− 1	− 3	− 20	− 21	− 21
Nasiriyah	− 7	− 6	− 8	− 2	− 1	− 3	− 18	− 20	− 31
Zakho	− 39	− 39	− 38	− 47	− 52	− 45	− 48	− 58	− 44
Sulaymaniyah	− 58	− 58	− 58	− 58	− 59	− 63	− 59	− 62	− 68
Salah ad Din	− 35.9	− 36	− 35.1	− 38.5	− 43.3	− 44.4	− 38.2	− 42.1	− 46.5
Al-Mosul	− 17	− 18	− 18	− 19	− 21	− 23	− 20	− 26	− 37
Khanaqin	− 10	− 1 1	− 10	− 20	− 24	− 27	− 15	− 21	− 33
Kirkuk	− 5	− 3	− 5	− 1	− 9	− 1 0	− 1	− 7	− 14

all stations except Basra where the Tmin was projected to decrease. The minimum change in Tmin was 1 °C in Nasiriyah during the first period and maximum increase of 6.7 °C under RCP8.5 in Sulaymaniyah (Table 11 and Fig. 5). On the other side, precipitation was projected to decrease across all the evaluated stations. The maximum decrease was − 68% under RCP8.5 in Sulaymaniyah during the third period and the minimum decrease was − 1% (Table 12 and Fig. 6).

Discussion

The statistical downscaling model shows a superior performance in modeling daily precipitation and temperature across the 12 studied stations in Iraq with a slight difference in performance among stations. Hessami et al. (2008) argued that "the agreement of simulations with observations depends on the GCMs atmospheric variables used as "predictors" in the regression-based approach, and the performance of the statistical downscaling model varies for different stations and season." The downscaling procedure of precipitation and temperature of this study was in agreement with other studies (e.g., Wilby et al. 1998; Huth 2002; Gachon et al. 2005), where they proved that using circulation variables (exemplified by geopotential, vorticity, or the wind component) and temperature (exemplified by geopotential heights at various levels and specific/relative humidity near the midtroposphere and specific/relative humidity) are superior in establishing a satisfactory relationship to that of any single predictor when downscaling temperature and/or precipitation. Presumably, the SDSM would receive more attention in future studies inside Iraq among the other downscaling methods

because of "less preprocessing requirements and computational costs" (Tavakol-Davani et al. 2013) in addition to the simplicity in implementation.

The outcomes from this study pointed an increase in temperatures and decrease in precipitation across the country. The greatest increase in annual maximum temperature was detected in Sulaymaniyah station in the north of Iraq at the end of the century 2080s under RCP8.5. While the lowest increase in maximum temperature was in Basrah station at 2020s. On the other hand, the greatest increase in minimum temperature was observed in Salah ad Din station (186 km to the north of Baghdad) at 2080s under RCP8.5. The lowest increase in minimum temperature was found in Nasiriyah (station in the south of Baghdad) at 2020s under RCP2.5. Surprisingly, Basrah station recorded a decrease in the minimum temperature during the three future periods except a slight increase at 2080s under RCP8.5. This could be attributed to the fact that warm and cold gulf currents can affect the climate of coastal regions when the winds pass across. Warm/cold currents heat/cool off the air temperatures over the gulf and bring higher/lower temperatures over land.

With respect to precipitation, the results show that the decrease in annual precipitation is more remarkable in the northern stations (Sulaymaniyah, Salah ad Din, and Zakho) than those in the southern part of the country. The greatest decrease in annual precipitation was observed in Sulaymaniyah at the end of 2080s under RCP8.5. While, the lowest decrease was detected in Najaf station. Although the general trend tends towards a decrease in precipitation across the country, some stations like Kirkuk and Al-Hay show a slight increase in the annual precipitation during the 2020s and 2040s, respectively. Such unforeseen trend is physically uninterpretable especially that most of the surrounded stations show decreasing of the

same periods. However, the uncertainty in measurements and modeling results could be the essential reasons behind.

In arid areas, positive changes in temperature will undoubtedly accelerate the process of desertification (Abbasnia et al. 2016) which in turn will ultimately affect on the agricultural activities in the Mesopotamia area. Therefore, this fact highlights the importance of swift adaptation and mitigation measures in the study area. The findings from this study are consistent with many other regional climate changes studies, e.g., in Iran (Najafi and Kermani 2016; Abbasnia et al. 2016), in UAE (Elhakeem et al. 2015), and in Kuwait (Al-Dousari 2005; Al-Awadhi 2014) where they reported an increase in temperature and dust storms and a decrease in precipitation. This was noted in the micro-features printed on surface of drifted sand particles from Iraq towards Kuwait (Al-Dousari and Al-Hazza 2013).

Conclusions

This study investigated the future projection climate change impacts on precipitation and temperature in several stations of Iraq. The NCEP/NCAR predictors were employed to calibrate and validate the SDSM along with the observed local station data. The CMIP5-CanESM2 outputs for the RCP8.5, RCP4.5, and RCP2.6 emission scenarios were used to projects the future changes. Based on the statistical metrics used in this study, results proved the superior performance of the SDSM in modeling present meteorological data. The downscaled results of the GCMs based on the calibrated SDSM showed that temperature would continue to increase in the future time slices. However, future precipitation will increase with more variability and uncertainty across the selected stations, but with consistent trend among RCPs. Overall, annual precipitation in CanESM2 will apparently decrease in the future. There is a clear trend of an increase in temperature and a decrease in precipitation in the study regions. Hence, the findings obtained from this study can be of use to help policy makers in making decisions and planning for adaptation of impacts of climate changes. Moreover, the results can provide a support for better water resources management in Iraq. It is planned to use the outcomes of this study to investigate the impacts of climate changes on water resources availability in Iraq in a further study.

Compliance with ethical standards

Conflict of interest   The authors declare that they have no conflict of interest.

References

Abbasnia M, Tavousi T, Khosravi M (2016) Assessment of future changes in the maximum temperature atselected stations in Iran based on HADCM3 and CGCM3 models. Asia-Pac J Atmos Sci 52(4):371–377

Al-Ansari NA, Ezz-Aldeen M, Knutsson S, Zakaria S (2012) Water harvesting and reservoir optimization in selected areas of south Sinjar Mountain, Iraq. J Hydrol Eng 18:1607–1616. https://doi.org/10.1061/(ASCE)HE.1943-5584.0000712

Al-Awadhi JM (2014) Measurement of air pollution in Kuwait City using passive samplers. ACS Journal 04(02):253–271

Al-Dousari A (2005) Causes and indicators of land degradation in the North-Western part of Kuwait. Arab Gulf J Sci Res 23(2):69–79

Al-Dousari AM, Al-Hazza A (2013) Physical properties of aeolian sediments within major dune corridor in Kuwait. Arab J Geosci 6(2):519–527

Al-Ghadban AN et al (1999) Preliminary assessment of the impact of draining of Iraqi marshes on Kuwait's northern marine environment. Part I. physical manipulation. Water Sci Technol 40(7):75–87

Al-Ghadban AN, Uddin S, Beg MU, Al-Dousari AM, Gevao B, Al-Yamani F (2008) Ecological consequences of river manipulations and drainage of Mesopotamian marshes on the Arabian Gulf ecosystem: investigations on changes in sedimentology and environmental quality, with special reference to Kuwait Bay. Kuwait Institute for Scientific Research (KISR) 9362:1–141

Al-Mukhtar M (2016) Modelling the root zone soil moisture using artificial neural networks, a case study. Environ Earth Sci 75(15):1124

Al-Mukhtar M (2018) Integrated approach to forecast future suspended sediment load by means of SWAT and artificial intelligence models, a case study. FOG Journal 51(Jun):52–77

Anandhi A, Shrinivas VV, Nanjundiah RS, Kumar DN (2009) Role of predictors in downscaling surface temperature to river basin in India for IPCC SRES scenarios using support vector machine. Int J Climatol 29(4):583–603

Christensen JH, Machenhauer B, Jones RG, Schär C, Ruti PM, Castro M, Visconti G (1997) Validation of presentday regional climate simulations over Europe: LAM simulations with observed boundary conditions. Clim Dyn 13:489–506

Chu J, Xia J, Xu CY, Singh V (2010) Statistical downscaling of daily mean temperature, pan evaporation and precipitation for climate change scenarios in Haihe River, China. Theor Appl Climatol 99(1):149–161. https://doi.org/10.1007/s00704-009-0129-6

Diaz-Nieto J, Wilby RL (2005) A comparison of statistical downscaling and climate change factor methods: impacts on low flows in the river Thames, United Kingdom. Clim Chang 69(2):245–268. https://doi.org/10.1007/s10584-005-1157-z

Elhakeem A, Elshorbagy WE, AlNaser H, Dominguez F (2015) Downscaling global circulation model projections of climate change for the United Arab Emirates. J Water Resour Plan Manag 141(9):04015007

Fowler HJ, Blenkinsop S, Tebaldi C (2007) Linking climate change modelling to impacts studies: recent advances in downscaling techniques for hydrological modelling. Int J Climatol 27(12):1547–1578. https://doi.org/10.1002/Joc.1556

Gachon P, St-Hilaire A, Ouarda TBM.J, Nguyen VTV, Lin C, Milton J, Chaumont D, Goldstein J, Hessami M, Nguyen TD, Selva F, Nadeau M, Roy P, Parishkura D, Major N, Choux M, Bourque A, (2005) A First Evaluation of the Strength and Weakenesses of Statistical Downscaling Methods for Simulating Extremes over Various Regions of Eastern Canada. Sub-component, Climate Change Action Fund (CCAF), Environment Canada, Montreal, Quebec, Canada, 209 pp

Gagnon S, Singh B, Rousselle J, Roy L (2005) An application of the statistical downscaling model (SDSM) to simulate climatic data

for streamflow modelling in Québec. Can Water Resour J 30(4): 297–314. https://doi.org/10.4296/cwrj3004297

Gebremeskel S, Liu YB, de Smedt F, Hoffmann L, Pfister L (2005) Analyzing the effect of climate changes on streamflow using statistically downscaled GCM scenarios. Int J River Basin Manag 2(4): 271–280. https://doi.org/10.1080/15715124.2004.9635237

Giorgi F (1990) Simulation of regional climate using a limited area model nested in a general circulation model. J Clim 3(9):941–963

Hassan Z, Shamsudin S, Harun S (2014) Application of SDSM and LARS-WG for simulating and downscaling of rainfall and temperature. Theor Appl Climatol 116(1–2):243–257

Hessami M, Gachon P, Ouarda TBMJ, St-Hilaire A (2008) Automated regression-based statistical downscaling tool. Environ Model Softw 23(6):813–834. https://doi.org/10.1016/j.envsoft.2007.10.004

Hewitson BC, Crane RG (1996) Climate downscaling: techniques and application. Clim Res 7(2):85–95

Huang J, Zhang J, Zhang Z, Xu C, Wang B, Yao J (2011) Estimation of future precipitation change in the Yangtze River basin by using statistical downscaling method. Stoch Env Res Risk A 25(6):781–792. https://doi.org/10.1007/s00477-010-0441-9

Huth R (2002) Statistical downscaling of daily temperature in Central Europe. J Clim 15(13):1731–1742. https://doi.org/10.1175/1520-0442(2002)015<1731:sdodti>2.0.co;2

IPCC (2013) In: Stocker TF, Qin D, Plattner GK, Tignor MM, Allen SK, Boschung J, Nauels A, Xia Y, Bex V, Midgley PM (eds) Climate change 2013: the physical science basis contribution of working group I to the fifth assessment report of the intergovernmental panel on climate change. Cambridge University Press, Cambridge, p 1535

Jones RG, Murphy JM, Noguer M (1995) Simulation of climate change over Europe using a nested regional climate model. I. Assessment of control climate, including sensitivity to location of lateral boundaries. Q J R Meteorol Soc 121(526):1413–1450. https://doi.org/10.1002/qj.49712152610

Khadka D, Pathak D (2016) Climate change projection for the Marsyangdi river basin, Nepal using statistical downscaling of GCM and its implications in geodisasters. Geoenvironmental Disasters 3:15. https://doi.org/10.1186/s40677-016-0050-0

Khan MS, Coulibaly P, Dibike Y (2006) Uncertainty analysis of statistical downscaling methods. J Hydrol 319(1–4):357–382. https://doi.org/10.1016/j.jhydrol.2005.06.035

Krause P, Boyle DP, Bäse F (2005) Comparison of different efficiency criteria for hydrological model assessment. Adv Geosci 5:89–97

Liu J, Williams JR, Wang X, Yang H (2009) Using MODAWEC to generate daily weather data for the EPIC model. Environ Model Softw 24(5):655–664. https://doi.org/10.1016/j.envsoft.2008.10.008

Moriasi DN, Arnold JG, Van Liew MW, Bingner RL, Harmel RD, Veith TL (2007) Model evaluation guidelines for systematic quantification of accuracy in watershed simulations. Trans ASABE 50(3):885–900

Moussa S, Sellami H, Mlayh A (2018) Climate change impact projections at the catchment scale in Tunisia using the multi-model ensemble mean approach. Arab J Geosci 11(8):181

Najafi R, Kermani M (2016) Uncertainty modeling of statistical downscaling to assess climate change impacts on temperature and precipitation. Earth Syst Environ 2:68. https://doi.org/10.1007/s40808-016-0112-z

Nash JE, Sutcliff JV (1970) River flow forecasting through conceptual models, part I—adiscussion of principles. J Hydrol 10:282–290

Nimah MN (2008) Water resources (2008) report of the Arab forum for environment and development. In: Tolba MK, Saab NW (eds) Arab environment and future challenges, Chapter 5. Arab Forum for Environment and Development, Cairo, pp 63–74

Romanowicz RJ, Bogdanowicz E, Debele SE, Doroszkiewicz J, Hisdal H, Lawrence D, Meresa HK, Napiórkowski JJ, Osuch M, Strupczewski WG, Wilson D (2016) Climate change impact on hydrological extremes: preliminary results from the polish-Norwegian project. Acta Geophys 64(2):477–509. https://doi.org/10.1515/acgeo-2016-0009

Singh J, Knapp HV, Arnold JG, Demissie M (2004) Hydrologic modeling of the Iroquois river watershed using HSPF and SWAT. J Am Water Resour Assoc 41(2):343–360

Tavakol-Davani H, Nasseri M, Zahraie B (2013) Improved statistical downscaling of daily precipitation using SDSM platform and data-mining methods. Int J Climatol 33:2561–2578

Wentz FJ, Ricciardulli L, Hilburn K, Mears C (2007) How much more rain will global warming bring? Science 317:233–235

Wetterhall F, Bárdossy A, Chen D, Halldin S, Xu C-Y (2009) Statistical downscaling of daily precipitation over Sweden using GCM output. Theor Appl Climatol 96(1):95–103. https://doi.org/10.1007/s00704-008-0038-0

Wilby RL, Dawson CW (2007) Statistical downscaling model (SDSM), version 4.2. Department of Geography, Lancaster University, Lancashire

Wilby RL, Wigley TML, Conway D, Jones PD, Hewitson BC, Main J, Wilks DS (1998) (1998). Statistical downscaling of general circulation model output: a comparison of methods. Water Resour Res 34: 2995–3008

Wilby RL, Hay LE, Gutowski WJ, Arritt RW, Takle ES, Pan Z, Leavesley GH, Martyn PC (2000) Hydrological responses to dynamically and statistically downscaled climate model output. Geophys Res Lett 27(8):1199. https://doi.org/10.1029/1999GL00607.

Wilby RL, Dawson CW, Barrow EM (2002) SDSM—a decision support tool for the assessment of regional climate change impacts. Environ Model Softw 17(2):145–157. https://doi.org/10.1016/s1364-8152(01)00060-3

Wilby RL, Whitehead PG, Wade AJ, Butterfield D, Davis RJ, Watts G (2006) Integrated modelling of climate change impacts on water resources and quality in a lowland catchment: river Kennet, UK. J Hydrol 330(1–2):204–220. https://doi.org/10.1016/j.jhydrol.2006.04.033

Wilks DS, Wilby RL (1999) The weather generation game: a review of stochastic weather models. Prog Phys Geogr 23:329–357. https://doi.org/10.1177/030913339902300302

Xu C-Y (1999) Climate change and hydrologic models: a review of existing gaps and recent research developments. Water Resour Manag 13(5):369–382. https://doi.org/10.1023/a:1008190900459

Yang T, Li H, Wang W, Xu C-Y, Yu Z (2012) Statistical downscaling of extreme daily precipitation, evaporation, and temperature and construction of future scenarios. Hydrol Process 26(23):3510–3523

Zakaria S et al (2013) Estimation of annual harvested runoff at Sulaymaniyah governorate, Kurdistan region of Iraq. Nat Sci 05(12):1272–1283